Clinical, Cosmetic and Investigational Dermatology

Dovepress
Taylor & Francis Group

Open Access Full Text Article

ORIGINAL RESEARCH

# The ceRNA Regulatory Network in Vitiligo: Evidence from Bioinformatics Analysis

Hedan Yang[1,*], Xiuzhen Li[2,*], Xiaoli Zhang[1], Yiping Ge[1], Yin Yang[1], Tong Lin[3]

[1]Department of Cosmetic Laser Surgery, Hospital of Dermatology, Chinese Academy of Medical Sciences and Peking Union Medical College, Nanjing, 210042, People's Republic of China; [2]Department of Cosmetic Laser Surgery, Hospital for Skin Diseases, Institute of Dermatology, Chinese Academy of Medical Sciences & Peking Union Medical College, Nanjing, 210042, People's Republic of China; [3]Jiangsu Key Laboratory of Molecular Biology for Skin Diseases and STIs, Hospital of Dermatology, Chinese Academy of Medical Sciences and Peking Union Medical College, Nanjing, 210042, People's Republic of China

*These authors contributed equally to this work

Correspondence: Tong Lin, Jiangsu Key Laboratory of Molecular Biology for Skin Diseases and STIs, Hospital of Dermatology, Chinese Academy of Medical Sciences and Peking Union Medical College, Nanjing, 210042, People's Republic of China, Email ddlin@hotmail.com; Yin Yang, Department of Cosmetic Laser Surgery, Hospital of Dermatology, Chinese Academy of Medical Sciences and Peking Union Medical College, Nanjing, 210042, People's Republic of China, Email yushiyy@163.com



**Background:** Vitiligo is an acquired depigmentary disorder caused by the loss of functional melanocytes. Increasing evidence suggests that competing endogenous RNA (ceRNA) interactions participate in this process, yet their global architecture in vitiligo remains unclear.
**Objective:** To delineate a long non-coding RNA (lncRNA)-microRNA (miRNA)-mRNA ceRNA network associated with vitiligo and to identify blood-borne RNA markers with diagnostic potential.
**Methods:** miRNA, mRNA, and lncRNA expression data from vitiligo patients and healthy controls were obtained from the GEO database (GSE141655 and GSE186928). Differentially expressed (DE) mRNAs, miRNAs and lncRNAs were screened ($|\log_2 FC| > 0.5$, adj. $p < 0.05$). Functional enrichment, STRING-based protein–protein interaction (PPI) mapping, and lncRNA–mRNA co-expression analysis (Pearson $r > 0.9$) was performed. miRNA–mRNA pairs were predicted with miRWalk 3.0, and miRNA–lncRNA pairs with miRanda v3.3a (score ≥ 140, energy ≤−20 kcal $mol^{-1}$). Triplets that shared the same miRNA, displayed positive lncRNA—mRNA correlation, and showed inverse expression relative to the miRNA were combined into a ceRNA network; hub nodes were ranked by degree centrality. Candidate lncRNAs were validated by RT-qPCR in peripheral blood from 20 vitiligo patients and 20 matched controls.
**Results:** A total of 454 DE-mRNAs (341 down-, 113 up-regulated), 22 DE-miRNAs (6 down-, 16 up-regulated), and 281 DE-lncRNAs (112 down-, 169 up-regulated) were identified. Enrichment analysis highlighted pathways linked to melanogenesis, oxidative stress, PI3K–Akt, JAK–STAT and IL-17 signalling. The ceRNA network comprised 33 lncRNAs, 12 miRNAs and 58 mRNAs; SLC32A1, GRIA2, PRKACG and WNT1 were top hub proteins in the PPI sub-network. Blood validation confirmed up-regulation of CASC19, NUCB1-AS1 and LINC01485 and down-regulation of VAV3–AS1, SPATA13–AS1, ZNF350–AS1 and LINC00677 (all $p < 0.05$).
**Conclusion:** Our findings map a vitiligo-related ceRNA landscape and pinpoints seven circulating lncRNAs with diagnostic promise. The results provide a foundation for probing non-coding RNA-mediated mechanisms and developing targeted therapies for vitiligo.
**Keywords:** vitiligo, ceRNA, lncRNA, bioinformatics

## Introduction

Vitiligo is a relatively common acquired pigmentary disorder characterized by a deficiency of melanocytes.[1] Despite proposed hypotheses including genetic, autoimmune, and oxidative stress mechanisms,[2,3] the precise pathogenesis remains elusive.

The role of different types of non-coding RNA in the pathogenesis of vitiligo has been demonstrated in previous studies. According to the competitive endogenous RNA (ceRNA) hypothesis, different types of RNA molecules—including mRNAs, lncRNAs, circRNAs, and pseudogenes—can regulate one another by competing for binding to the same miRNAs via microRNA response elements (MREs). This interaction results in the formation of a ceRNA regulatory network that is involved in the regulation of various biological processes.[4] The circRNA-miRNA-mRNA regulatory network not only serves

https://doi.org/10.2147/CCID.S528604
Received: 18 March 2025
Accepted: 18 August 2025
Published: 30 August 2025

as a critical modulator of various functions of melanocytes,[5,6] but may also be an important regulatory factor in the onset and development of vitiligo.[7] Additionally, the ceRNA regulatory network is implicated in oxidative stress, which mediates melanocyte damage and contributes to the pathogenesis of vitiligo.[8] Furthermore, the ceRNA network is involved in α-MSH-induced melanin synthesis and may serve as a potential therapeutic target for skin pigmentation disorders.[9] While existing studies have suggested the potential role of ceRNA networks in regulating melanocyte function and their possible involvement in vitiligo pathogenesis, systematic investigations remain limited. In this study, we aimed to employ bioinformatics to analyze the role of the ceRNA regulatory network in the pathogenesis of vitiligo to explore potential molecular targets.

# Materials and Methods

## miRNA and mRNA/lncRNA Data Sets

The miRNA expression profiling data were sourced from the NCBI GEO database, specifically dataset GSE141655, which includes blood samples from 10 vitiligo patients and 10 healthy individuals. Additionally, mRNA and lncRNA data were obtained from the NCBI GEO database, dataset GSE186928, comprising plasma exosomes samples from 5 vitiligo patients and 5 healthy controls.

## Differential Screening of mRNA, lncRNA, and miRNA

In the GSE141655 dataset, we used the classical Bayesian method provided by the limma package (version 3.10.3, WEHI, Melbourne, VIC, Australia) to perform differential miRNA analysis between vitiligo patients and control groups.[10] In the GSE186928 dataset, we used the edgeR package (version 3.40.1, WEHI, Melbourne, VIC, Australia) to perform differential mRNA and lncRNA analysis between vitiligo patients and control groups, and obtained the corresponding $p$-values and log2 fold change ($\log_2$ FC) values.[11] The threshold for differential expression was set as follows: miRNA/mRNA/lncRNA: $p < 0.05$ and $|\log_2 FC| > 0.5$.

## Functional Enrichment and Pathway Analysis of Differentially Expressed mRNAs

Functional enrichment analysis of the above-mentioned differentially expressed genes was performed using the bioinformatics tool DAVID (version 6.8, Laboratory of Human Retrovirology and Immunoinformatics, Frederick National Laboratory for Cancer Research, Frederick, MD, USA),[12] based on the Gene Ontology (GO) categories: Biological Process (BP), Cellular Component (CC), Molecular Function (MF), as well as KEGG pathway. A significance threshold of $p < 0.05$ and a minimum count of enriched items (≥2) were established to determine significant enrichment results.

## Construction of the Protein-Protein Interaction (PPI) Network and Node Connectivity Analysis

To analyze potential interactions among genes encoding proteins, we utilized the STRING database (Version 11.0, STRING Consortium, Swiss Institute of Bioinformatics, Lausanne, Switzerland). The input gene set comprised DE-mRNAs, specifically from Homo sapiens. We set the PPI score threshold to 0.4 (indicating medium confidence), ensuring that only protein nodes associated with the identified up-regulated and down-regulated genes were included. Following the identification of PPI relationship pairs, we employed Cytoscape software (version 3.4.0, Cytoscape Consortium, CA, USA) to construct network visualizations. Node connectivity analysis was conducted using the CytoNCA plug-in (version 2.1.6, College of Computer Science & Electronic Engineering, Hunan University, Changsha, Hunan, China), with parameters configured to exclude weights. The results encompassed Degree Centrality (DC), allowing us to identify key nodes involved in protein interactions within the PPI network, specifically hub proteins, through a ranking based on node connectivity.

## Analysis of lncRNA and mRNA Co-Expression

We analyzed one-to-one matched samples of mRNA and lncRNA data to calculate the Pearson correlation coefficients for the DE-mRNAs and lncRNAs. Correlation tests were conducted, focusing on filtering pairs with a correlation coefficient (r) greater than 0.9 and $p < 0.05$, considering these mRNAs and lncRNAs to be significantly correlated, with mRNAs serving as potential target genes for lncRNAs.

## miRNA Prediction and Upstream lncRNA Prediction

DE-mRNAs were first subjected to target-site prediction in the miRWalk 3.0 database[13]. The resulting miRNA–mRNA pairs were intersected with the list of differentially expressed miRNAs (DE-miRNAs), and only overlapping miRNAs were retained, yielding DE-miRNA–DE-mRNA interaction pairs. For lncRNA–miRNA interactions, miRanda software (version 3.3a, Computational Biology Center, Memorial Sloan Kettering Cancer Center, New York, NY, USA) was employed with the parameters "-sc 140 -en −20" (ie, score ≥ 140 and free energy ≤ −20 kcal/mol). Predicted pairs were then filtered against the DE-miRNA list to obtain DE-miRNA–DE-lncRNA interaction pairs. These curated interaction sets were subsequently used to construct the ceRNA regulatory network.

## Construction of the ceRNA Network

Using the DE-miRNA–mRNA and DE-miRNA–lncRNA interaction pairs obtained above, we first extracted lncRNA–miRNA–mRNA interaction pairs that were governed by the same miRNA. Next, Pearson correlation analysis was performed on expression profiles of each lncRNA–mRNA pair; only positively co-expressed pairs ($r > 0.90$, $p < 0.05$) were retained. Considering the competitive binding model of ceRNAs, we further required that the miRNA show an inverse expression trend relative to its two targets. The resulting lncRNA-miRNA-mRNA interaction pairs were assembled into a ceRNA network. Node degree centrality was calculated with the CytoNCA plug-in of Cytoscape (settings: "without weight"). A higher degree indicates greater topological importance within the network.

## Pathway Enrichment Analysis of mRNAs in the ceRNA Network

In this section, we conducted an enrichment analysis of mRNA pathways within the previously established ceRNA network. We first selected both up-regulated and down-regulated mRNAs from the network and performed single-gene functional annotation using the DAVID enrichment analysis tool. This process identified the functional pathways associated with each mRNA. Subsequently, we integrated the lncRNA-miRNA-mRNA relationships identified in the ceRNA network to highlight key signaling pathways based on the annotation results of each mRNA. The selected pathways included the PI3K–Akt signaling pathway, JAK–STAT signaling pathway, IL-17 signaling pathway, TGF-β signaling pathway, cGMP–PKG signaling pathway, cAMP signaling pathway, and Ras signaling pathway. For each pathway, the top three up-regulated and top three down-regulated mRNAs with the highest degree values were selected. These key mRNAs, together with their upstream miRNAs and lncRNAs, were integrated to build a lncRNA–miRNA–mRNA–Pathway regulatory network, thereby highlighting pivotal pathways as well as their core mRNA and lncRNA regulators.

## Human Peripheral Blood Mononuclear Cells Isolation

The study was conducted in accordance with the Declaration of Helsinki, and was approved by the Ethics Committee of the Hospital of Dermatology, Chinese Academy of Medical Sciences (2022-KY-045), and all participants provided informed consent. A total of 20 blood samples were collected from patients with vitiligo and 20 healthy controls. Density gradient centrifugation was performed using Ficoll-Paque (Cytiva).

## RNA Extraction and RT-qPCR

All whole-blood RNA samples were re-labeled by a technician not involved in downstream analyses; the investigator performing RT-qPCR and data normalization was blinded to clinical status until after statistical analysis. Total RNA was extracted from blood samples using RNAiso Plus reagent (Takara, Japan). RT-qPCR were conducted using Evo M-MLV RT Master Mix and SYBR Green Pro Taq HS Pre (Takara, Japan). The primer sequences utilized in this study are listed in Table 1. The equipment used was LightCycler 480.

## Statistical Analysis

Statistical analyses were performed using R software (version 4.1.1, R Foundation for Statistical Computing, Vienna, Austria) and GraphPad Prism 5 (GraphPad Software, Inc., San Diego, CA, USA). RT-qPCR tests were conducted in

**Table 1** Primers Used in This Study

| Primer | Forward | Reverse |
|---|---|---|
| NUCB1-AS1 | TGCTCATCCAGGACACCATC | CCTCAGGTGTTGGACTCTTCC |
| CASC19 | GAGGAGGAAGGCAGCACAAT | GGTTCTAACCCAGGCACTCC |
| USP2-AS1 | GGAACTCACAACACACGGGA | TTGCACAAGATGACAGGGCT |
| KCNK4-TEX40 | GGTGTATCCCTCACAGCACC | AGCAATTCCACACCCACTCG |
| LINC01518 | TGAAACCTGTCACTGCCACC | TGGTACTGTTCCGTCACTGC |
| LINC01387 | GAGGTCTTCTCCCAGAAGCG | GCGGCAGCTTAATTCCAAGG |
| LINC01299 | AGGTCCTGGGGTATCCTCTG | GTGAGCTGCACAACTCAGGA |
| LINC01630 | GCCCCACTTTCTGCCACTAT | GAATCTCAGCCACGTTTGCC |
| LINC01485 | GAGAGAGCACTTTCGGGCTT | CTTGCCACGCTCACAATCTG |
| ZNF350-AS1 | ATTCTGTCGTCTGGGAACGG | GCACGGACCTAGGTGGAATC |
| VAV3-AS1 | AGATGGGATGGTTGTGCCTG | GGGTCATGTGTGAGCTGCTA |
| LINC00677 | GCGTAAATGCGGAAAGGTGA | CTAGGAACCCCACTCCGCTA |
| LINC01465 | GGCCGTGGTTTGAAGTTTCC | CTTTCCCGCCTGTTTTCTGC |
| SPATA13-AS1 | GATGGGACGCAAGCTCTGAA | ACCCTTGCCTTCCTTGGTTT |
| PSD2-AS1 | CCCACCACCCCTGATACCTA | TGCCCCCTCAAACCATTGAA |

triplicate or more. GraphPad Prism was employed for data analysis and for analysis and visualization. To identify differences between groups, the Student's *t*-test was utilized, with a significance threshold set at $p < 0.05$.

# Results

## Differential Expression and Functional Enrichment Analysis

Using datasets GSE141655 and GSE186928, we examined 2588 miRNAs, 19233 mRNAs and 9866 lncRNAs. With the criteria $|\log2\ FC| > 0.5$ and $p < 0.05$, 454 differentially expressed mRNAs (DE-mRNAs; 113 up- and 341 down-regulated), 22 DE-miRNAs (16 up, 6 down) and 281 DE-lncRNAs (169 up, 112 down) were obtained (Figure 1A–C).

Subsequently, Gene Ontology (GO) function enrichment analysis and Kyoto Encyclopedia of Genes and Genomes (KEGG) pathway enrichment analysis were conducted on the DE-mRNAs to investigate their potential biological functions. The GO functional enrichment analysis of down-regulated mRNAs revealed significant associations with proteolysis and cell adhesion (biological process, BP), as well as integral components of membranes and plasma membranes (cellular component, CC). KEGG pathway analysis indicated that these mRNAs primarily participate in neuroactive ligand-receptor interactions and vascular smooth muscle contraction (Figure 2A and C). In contrast, the GO functional enrichment analysis of up-regulated mRNAs was predominantly linked to intermediate filament organization and fertilization (biological process, BP), neuron projection extracellular matrix (cellular component, CC), along with signaling receptor activity and cell adhesion molecule binding (molecular function, MF) (Figure 2B).

## Protein–Protein Interaction (PPI) Network Analysis

To investigate potential interactions among proteins encoded by DE-mRNAs, we utilized the STRING database to assess the node connectivity within protein interaction networks. We identified a total of 544 protein interaction pairs and

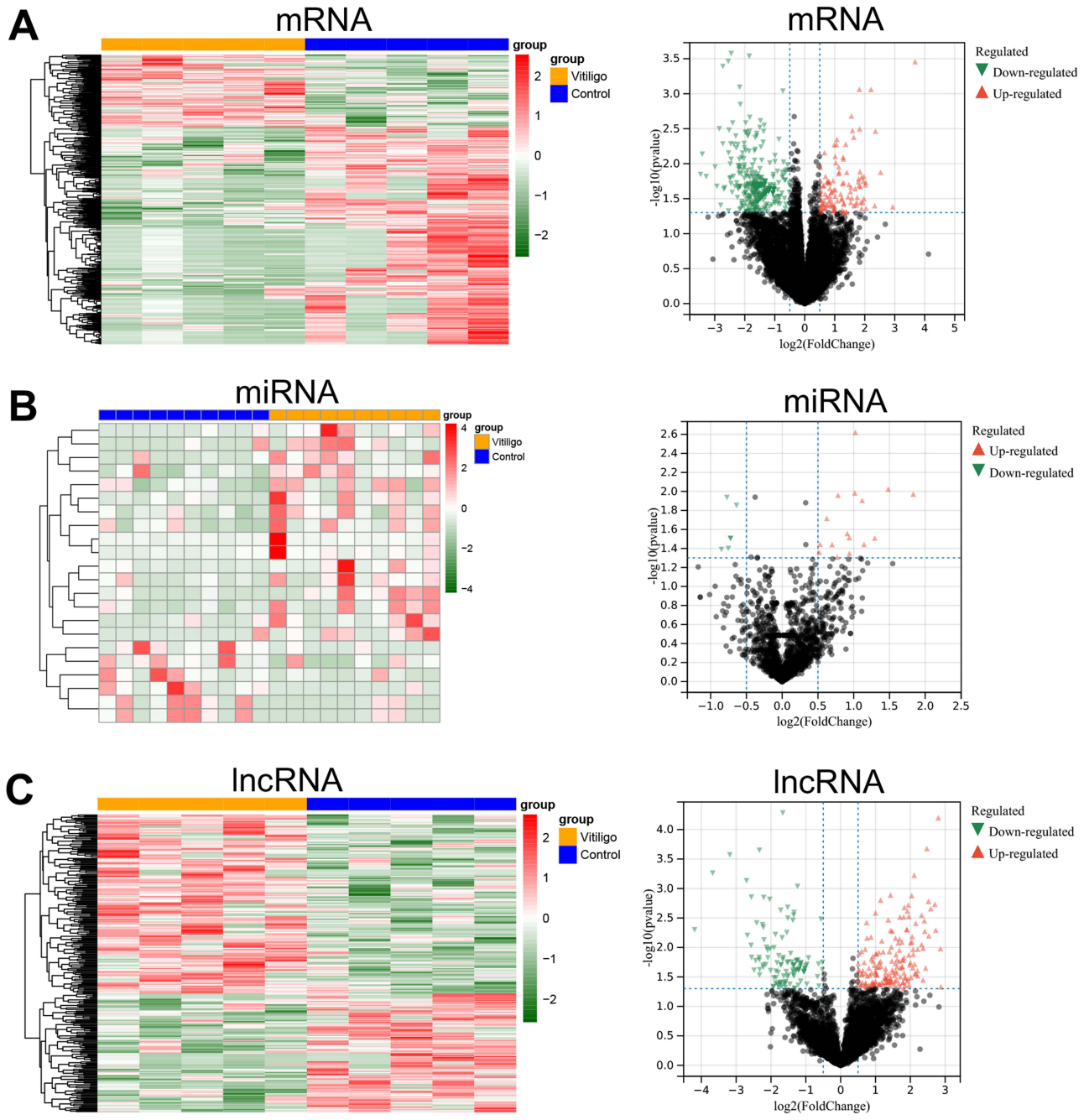


**Figure 1** Heat map and volcano diagram of the expression profiles of differentially expressed RNAs. (**A**) Expression profiles of differentially expressed mRNAs; (**B**) Expression profiles of differentially expressed miRNAs; (**C**) Expression profiles of differentially expressed lncRNAs.

constructed the network using Cytoscape software. The network contained 271 nodes, and the top 15 hub proteins ranked by degree were SLC32A1, GRIA2, PRKACG, PTGS2, CYP2C9, RHO, WNT1, CYP1A2, OTX2, TH, NTRK2, CYP2A6, CYP4F2, GAP43, and OPALIN (Figure 3A).

## mRNA and lncRNA Co-Expression Analysis

To examine the interactions between differentially expressed mRNAs and lncRNAs, we conducted a co-expression analysis. A total of 798 significant co-expression pairs were identified based on Pearson analysis ($r > 0.9$ and $p < 0.05$), which included 385 mRNAs and 84 lncRNAs, suggesting that the mRNAs may serve as potential target genes for these lncRNAs.


https://doi.org/10.2147/CCID.S528604

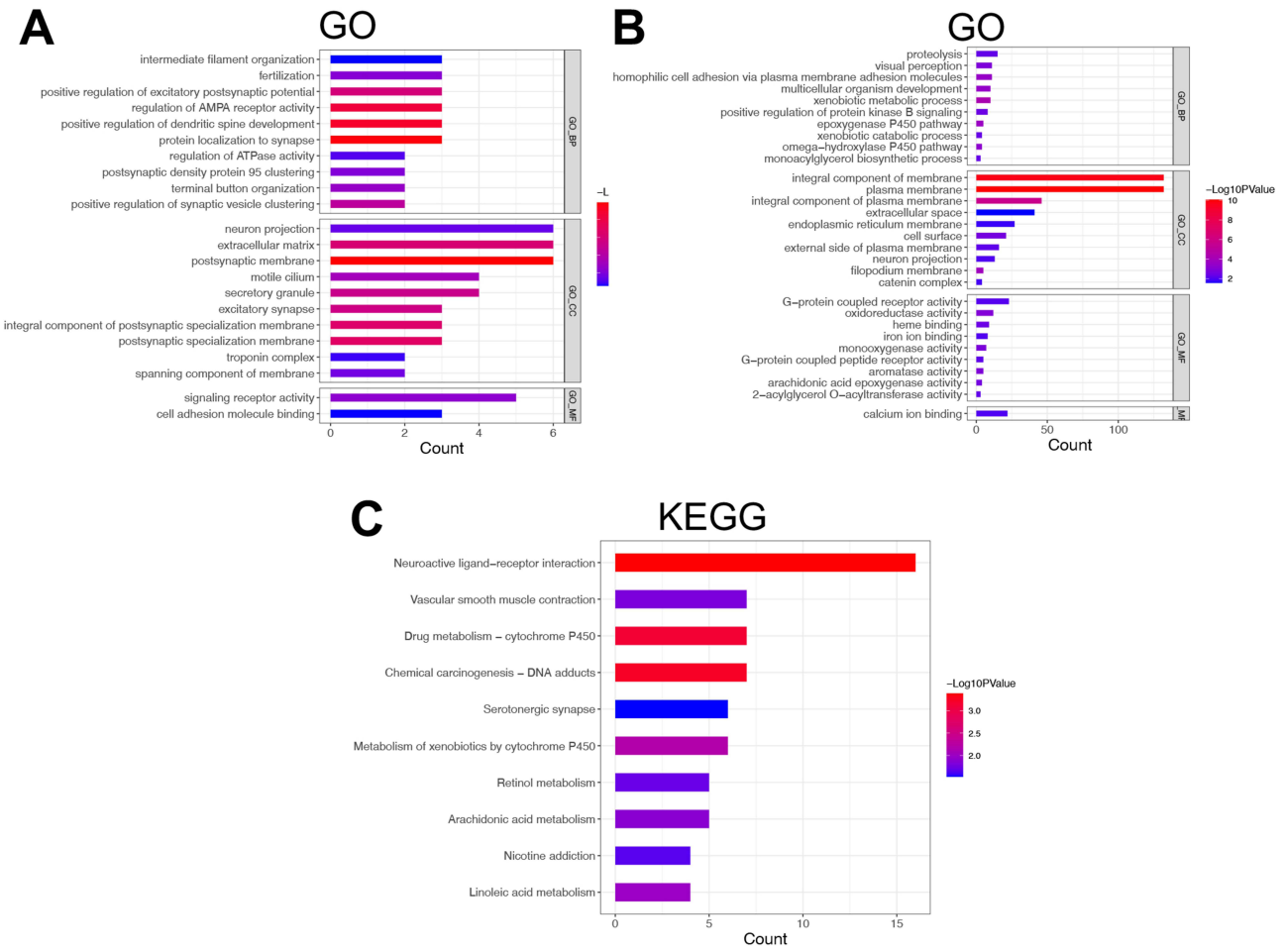


**Figure 2** GO and KEGG analysis of differentially expressed mRNAs. (**A**) GO analysis of up-regulated mRNAs; (**B**) GO analysis of down-regulated mRNAs; (**C**) KEGG analysis of down-regulated mRNAs.

## Prediction Analysis of miRNA Target Genes and Upstream lncRNAs

Using the DE-mRNAs as a foundation, miRNA prediction was conducted through miRwalk. This analysis yielded 702 miRNA-mRNA, interaction pairs (20 miRNAs, 277 mRNAs), following the intersection with the DE-miRNAs. Additionally, based on the differentially expressed miRNAs and lncRNAs, a total of 702 lncRNA-miRNA interaction pairs (19 miRNAs, 69 lncRNAs) were predicted.

## ceRNA Network Analysis

Building on the previously identified lncRNA-miRNA and miRNA-mRNA relationship pairs, we filtered for miRNA-lncRNA-mRNA triplet relationships regulated by the same miRNA to construct the ceRNA network (Figure 3B). Triplets sharing the same miRNA were kept only when (i) the lncRNA and mRNA were positively correlated ($r > 0.9$) and (ii) their expression direction was opposite to that of the miRNA. The final ceRNA network contained 33 lncRNAs, 12 miRNAs and 58 mRNAs connected by 82 lncRN-miRNA interaction pairs, 75 miRN-mRNA interaction pairs and 103 lncRNA-mRNA interaction pairs.

## Pathway Enrichment Analysis of lncRNAs and miRNAs

We obtained pathway annotation results for three up-regulated mRNAs (CSF3, INHBE, NPR1) and three down-regulated mRNAs (NLGN1, PLA2G2D, KCNMA1). By integrating these findings with the previously mentioned ceRNA network relationship pairs, we identified a total of 168 lncRNA-miRNA-mRNA-pathway regulatory mechanism relationship pairs

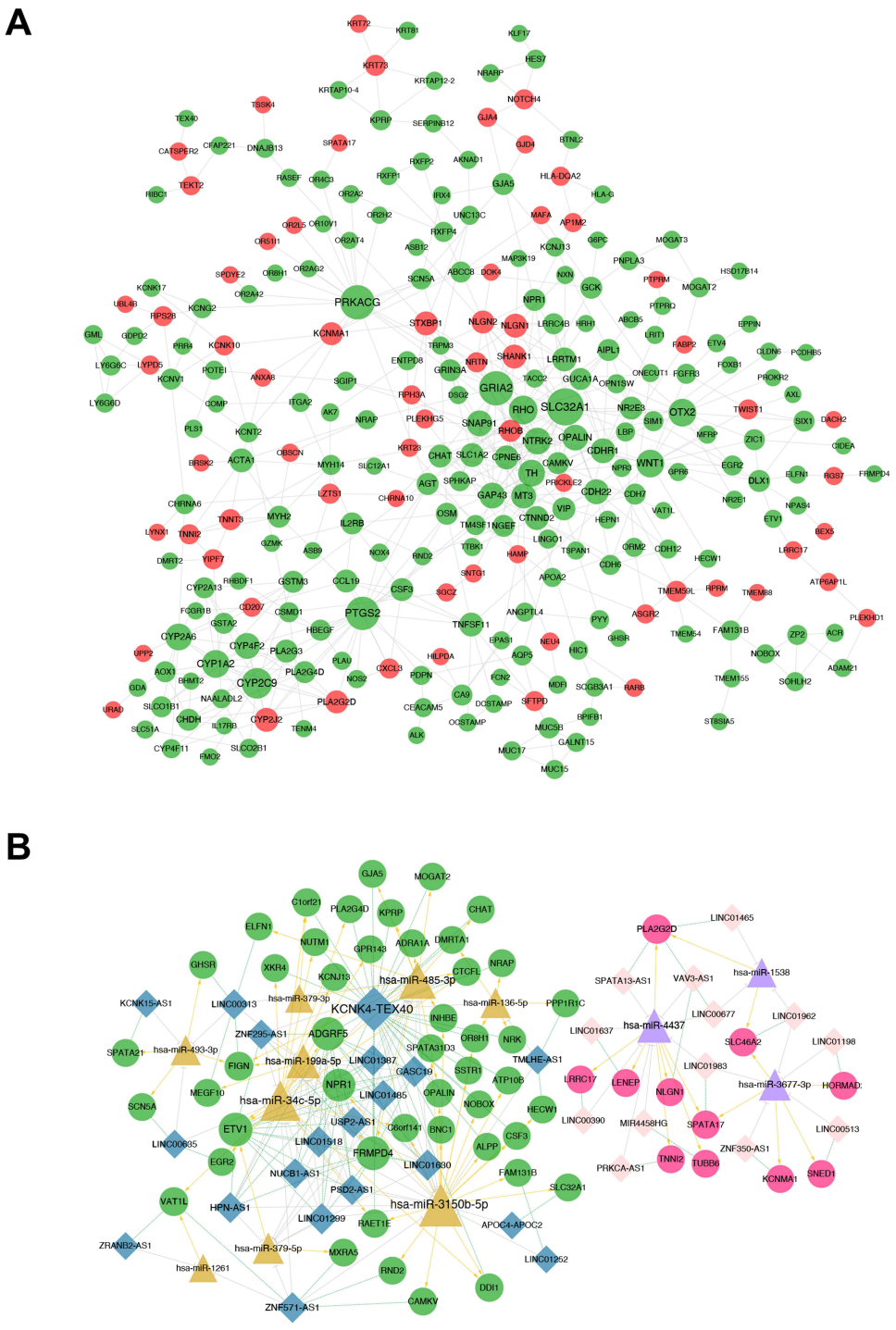


**Figure 3** (**A**) Protein Interaction Network Construction (PPI) analysis (red represents up-regulated proteins, green represents down-regulated proteins, gray connecting lines represent protein interactions, and node size represents connectivity size); (**B**) ceRNA network diagram (red circles represent up-regulated mRNAs, green circles represent down-regulated mRNAs; yellow triangles represent up-regulated miRNAs, purple triangles represent down-regulated miRNAs; blue rhombuses represent down-regulated lncRNAs, pink rhombuses represent up-regulated lncRNAs; grey T-links represent miRNA-lncRNA regulatory relationships, yellow arrows represent miRNA-mRNA regulatory relationship, green dashed line represents mRNA and lncRNA co-expression relationship).

(Figure 4). This dataset comprises 16 lncRNAs, 5 miRNAs, 6 mRNAs, and 28 pathways. Notably, significant annotations were found for several key signaling pathways, including the PI3K–Akt signaling pathway, JAK–STAT signaling pathway, IL-17 signaling pathway, TGF–β signaling pathway, cGMP–PKG signaling pathway, cAMP signaling pathway, and Ras signaling pathway.


https://doi.org/10.2147/CCID.S528604

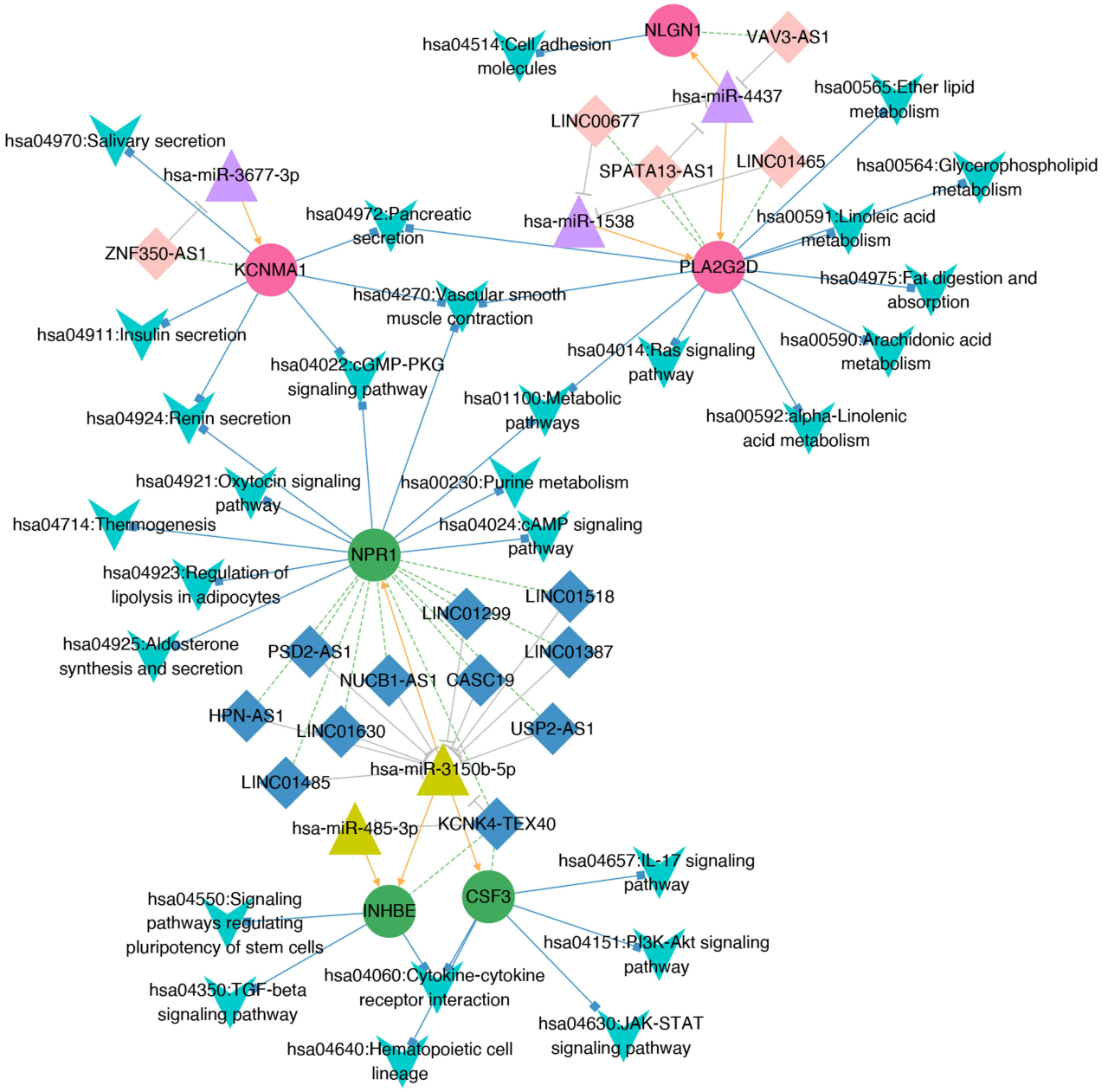


**Figure 4** lncRNA–miRNA–mRNA–Pathway regulatory network diagram (where V-shaped nodes represent pathway, red circles represent up-regulated mRNAs, green circles represent down-regulated mRNAs; yellow triangles represent up-regulated miRNAs, purple triangles represent down-regulated miRNAs; blue rhombuses represent down-regulated lncRNAs, pink rhombuses represent up-regulated lncRNA; gray T-shaped connecting lines represent miRNA–lncRNA regulatory relationships, yellow arrows represent miRNA–mRNA regulatory relationships, green dashed lines represent mRNA and lncRNA co-expression relationships, and blue square connecting lines represent mRNA-pathway regulatory relationships).

## Validation of lncRNA Expression in Blood Samples from Vitiligo Patients

To assess the reliability of our data analysis results, we conducted a validation study on the expression levels of the aforementioned 16 lncRNAs in blood samples from 20 vitiligo patients and from 20 healthy controls. Excluding the 2 lncRNAs with missing primers, 7 of the remaining 14 validated lncRNAs were consistent with our bioinformatic analysis results. Specifically, CASC19, NUCB1–AS1, and LINC01485 exhibited elevated expression levels in the blood of vitiligo patients, whereas VAV3–AS1, SPATA13–AS1, ZNF350–AS1, and LINC00677 demonstrated reduced expression levels (Figure 5).

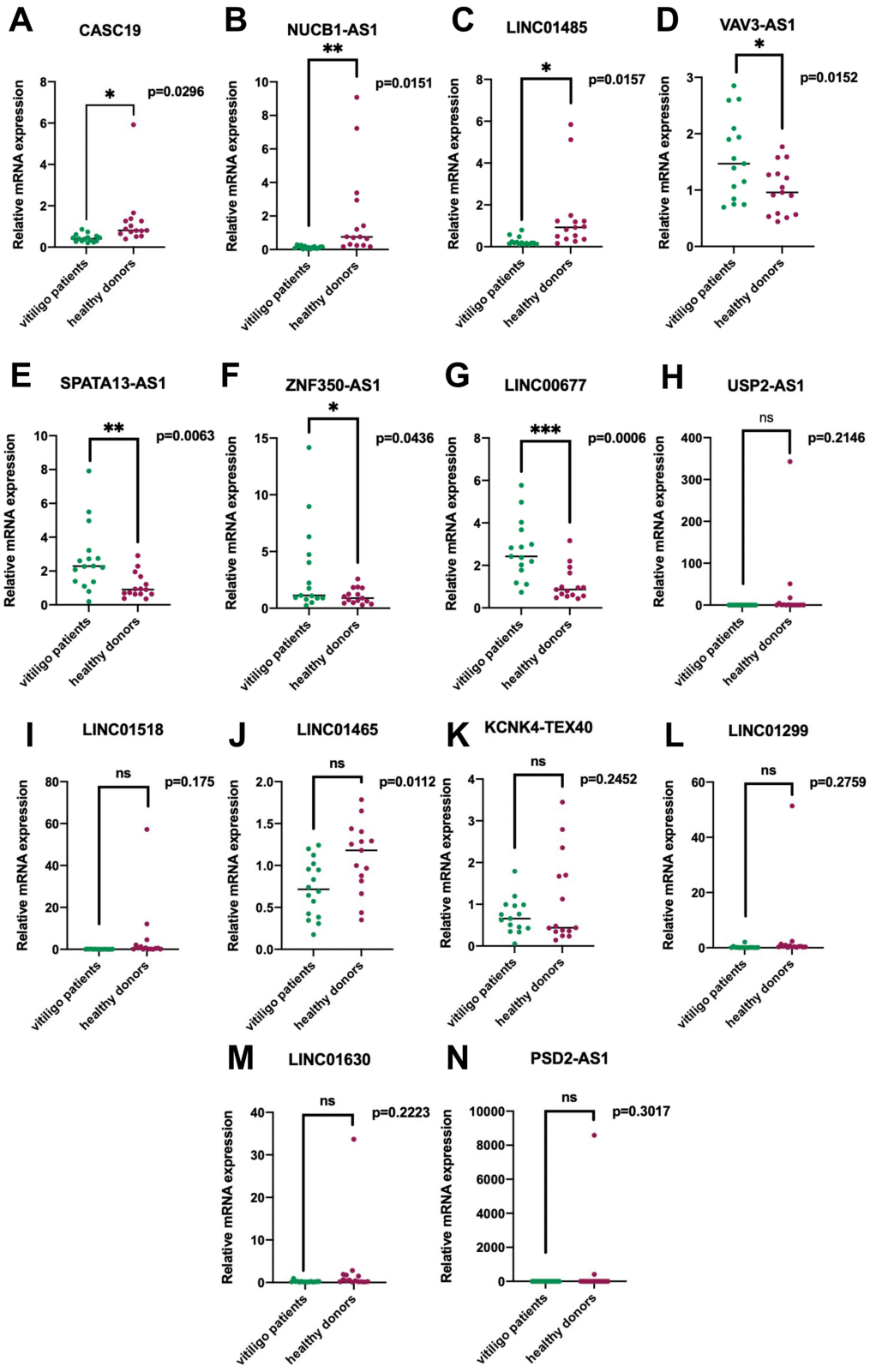


**Figure 5** lncRNA expression in blood samples from a total of 20 vitiligo patients and 20 healthy individuals. Seven lncRNAs were consistent with the results of bioinformatic analysis. (**A**) The expression level of CASC19 in the blood of vitiligo patients is higher than that in healthy individuals; (**B**) NUCB1–AS1 is also up-regulated in vitiligo patients; (**C**) LINC01485 had elevated expression in the blood of vitiligo patients; (**D**) The expression level of VAV3–AS1 in the blood of vitiligo patients is lower than that in healthy individuals; (**E**) SPATA13–AS1 levels are reduced in vitiligo; (**F**) ZNF350–AS1 expression is likewise decreased in vitiligo patients; (**G**) LINC00677 is significantly down-regulated in vitiligo patient blood; (**H**–**N**) USP2–AS1, LINC01518, LINC01465, KCNK4–TEX40, LINC01299, LINC01630, and PSD2–AS1 show no statistically significant difference between vitiligo patients and healthy individuals. (ns: $p \geq 0.05$; *$p < 0.05$; **$p < 0.01$; ***$p < 0.001$).


https://doi.org/10.2147/CCID.S528604

## Discussion

In this study, constructed a lncRNA–miRNA–mRNA ceRNA network and confirmed seven dysregulated lncRNAs in an independent cohort. The data support a model in which aberrant ceRNA crosstalk contributes to melanocyte loss through pathways related to immune activation and oxidative stress.

Differential analysis identified 281 lncRNAs, 22 miRNAs and 454 mRNAs that are significantly altered in vitiligo blood. Enrichment pointed to pathways previously implicated in the disease—PI3K–Akt, JAK–STAT, IL–17, TGF–β, cAMP/cGMP and Ras signalling—highlighting immune activation, cytokine response and redox imbalance.[2,14,15] Integrating target prediction, co-expression and inverse miRNA–target regulation produced a ceRNA network composed of 33 lncRNAs, 12 miRNAs and 58 mRNAs. Hub analysis placed SLC32A1, GRIA2, PRKACG and WNT1 at central positions, suggesting a potential link between neurotransmission, cAMP signalling and melanocyte survival.[16,17] RT–qPCR confirmed up-regulation of CASC19, NUCB1–AS1 and LINC01485 and down-regulation of VAV3–AS1, SPATA13–AS1, ZNF350–AS1 and LINC00677 in patient blood, nominating them as circulating biomarkers. Vitiligo pathogenesis is driven by autoimmune attack and oxidative damage to melanocytes. The identified pathways fit this paradigm: PI3K–Akt and JAK–STAT govern cytokine signalling and T-cell activation; their dysregulation supports the autoimmune component of vitiligo. IL-17 and TGF–β pathways modulate Th17/Treg balance and inflammation in skin. cAMP/cGMP signalling regulates melanogenesis and antioxidant defences. Within the ceRNA network, although several of these lncRNAs were first described in cancer,[18–22] their documented roles in proliferation, immune modulation and oxidative stress provide plausible links to melanocyte dysfunction.

The seven validated lncRNAs are detectable in peripheral blood, making them attractive, minimally invasive candidates for early diagnosis or for monitoring disease activity. In addition, miRNA or lncRNA mimics/antagonists directed at the highly connected nodes of the ceRNA network could represent novel therapeutic avenues.

Our study has several limitations. First, both the sample size in the database and the number of clinical samples used to validate the results of our bioinformatics analysis are relatively small; therefore, additional clinical samples and independent validation in a multi-center cohort are necessary to substantiate our findings. Second, blood profiles may not fully reflect lesional skin biology, paired skin–blood studies are required. Finally, while our bioinformatics analysis provides preliminary insights into ceRNA involvement in vitiligo pathogenesis, functional experiments are required to test thecausal relationships between the identified ceRNA nodes and melanocyte survival.

## Conclusion

In conclusion, our integrative analysis reveals a blood-based ceRNA network that converges on immune and oxidative pathways central to vitiligo. The seven dysregulated lncRNAs provide a springboard for mechanistic studies and may evolve into clinically useful biomarkers or therapeutic targets.

## Ethics Statement

This study was approved by the Ethics Committee of Institute of Dermatology, Chinese Academy of Medical Sciences and Peking Union Medical College (2022-KY-045).

## Acknowledgments

This work was supported by the CAMS Innovation Fund for Medical Sciences (CIFMS-2021-I2M-1-001) and Funds for Science and Technology Plan Projects in Jiangsu Province (BE2023675).

## Funding

CAMS Innovation Fund for Medical Sciences (CIFMS-2021-I2M-1-001) sponsored the study. Funds for Science and Technology Plan Projects in Jiangsu Province (BE2023675).

## Disclosure

The authors declare no conflicts of interest in this work.

## References


1. Premkumar M, Bhaskar Kalarani I, Mohammed V, et al. An extensive review of vitiligo-associated conditions. *Int J Dermatol Venereol*. 2024;7(1):44–51. doi:10.1097/JD9.0000000000000346
2. Speeckaert R, Caelenberg EV, Belpaire A, et al. Vitiligo: from pathogenesis to treatment. *J Clin Med*. 2024;13(17):5225. doi:10.3390/jcm13175225
3. Upadhya S, Andrade MJ, Shukla V, et al. Genetic and immune dysregulation in vitiligo: insights into autoimmune mechanisms and disease pathogenesis. *Autoimmun Rev*. 2025;24:103841. doi:10.1016/j.autrev.2025.103841
4. Chen B, Tan L, Wang Y, et al. LOC102549726/miR-760-3p network is involved in the progression of ISO-induced pathological cardiomyocyte hypertrophy via endoplasmic reticulum stress. *J Mol Histol*. 2023;54(6):675–687. doi:10.1007/s10735-023-10166-1
5. Feghahati FS, Ghafouri-Fard S. A comprehensive outline of the role of non-coding RNAs in vitiligo. *Biochem Biophys Rep*. 2025;41:101916. doi:10.1016/j.bbrep.2025.101916
6. Zhu Z, Ma Y, Li Y, et al. The comprehensive detection of miRNA, lncRNA, and circRNA in regulation of mouse melanocyte and skin development. *Biol Res*. 2020;53(1):4. doi:10.1186/s40659-020-0272-1
7. Li L, Xie Z, Qian X, et al. Identification of a potentially functional circRNA-miRNA-mRNA regulatory network in melanocytes for investigating pathogenesis of vitiligo. *Front Genet*. 2021;12:663091. doi:10.3389/fgene.2021.663091
8. Li S, Zeng H, Huang J, et al. Identification of the competing endogenous RNA networks in oxidative stress injury of melanocytes. *DNA Cell Biol*. 2021;40(2):192–208. doi:10.1089/dna.2020.5455
9. Jiang L, Huang J, Hu Y, et al. Identification of the ceRNA networks in α-MSH-induced melanogenesis of melanocytes. *Aging*. 2020;13(2):2700. doi:10.18632/aging.202320
10. Smyth G. *Limma: Linear Models for Microarray Data. Bioinformatics and Computational Biology Solutions Using R and Bioconductor*. Gentleman R, Carey V, Dudoit S, Irizarry R, Huber W, Edited by. New York: Springer; 2005.
11. Robinson MD, McCarthy DJ, Smyth GK. edgeR: a bioconductor package for differential expression analysis of digital gene expression data. *Bioinformatics*. 2010;26(1):139–140. doi:10.1093/bioinformatics/btp616
12. Huang DW, Sherman BT, Lempicki RA. Systematic and integrative analysis of large gene lists using DAVID bioinformatics resources. *Nat Protocols*. 2009;4(1):44–57. doi:10.1038/nprot.2008.211
13. Dweep H, Sticht C, Pandey P, et al. miRWalk–database: prediction of possible miRNA binding sites by "walking" the genes of three genomes. *J Biomed Inform*. 2011;44(5):839–847. doi:10.1016/j.jbi.2011.05.002
14. Chen L, Chen S, Li P, et al. Exploration of the mechanism of Qinglongyi-Buguzhi drug pair in treating vitiligo based on network pharmacology, molecular docking and experimental verification. *J Ethnopharmacol*. 2024;334:118595. doi:10.1016/j.jep.2024.118595
15. Maranduca MA, Cosovanu MA, Clim A, et al. The renin-angiotensin system: the challenge behind autoimmune dermatological diseases. *Diagnostics*. 2023;13(22):3398. doi:10.3390/diagnostics13223398
16. Bang J, Zippin JH. Cyclic adenosine monophosphate (cAMP) signaling in melanocyte pigmentation and melanomagenesis. *Pigment Cell Melanoma Res*. 2021;34(1):28–43. doi:10.1111/pcmr.12920
17. Steuer Costa W, Yu S-C, Liewald JF, et al. Fast cAMP modulation of neurotransmission via neuropeptide signals and vesicle loading. *Curr Biol*. 2017;27(4):495–507. doi:10.1016/j.cub.2016.12.055
18. Fishe JN, Labilloy G, Higley R, et al. Single nucleotide polymorphisms (SNPs) in PRKG1 & SPATA13-AS1 are associated with bronchodilator response: a pilot study during acute asthma exacerbations in African American children. *Pharmacogen Genom*. 2021;31(7):146–154. doi:10.1097/FPC.0000000000000434
19. Gao X, Wang G, Zhang M, et al. LINC01485 contributes to colorectal cancer progression by targeting miR −383-5p/ KRT80 axis. *Environ Toxicol*. 2024;39(1):398–408. doi:10.1002/tox.23983
20. Miramontes-Gonzalez JP, Usategui-Martín R, Martín-Vallejo J, et al. VAV3 rs7528153 and VAV3-AS1 rs1185222 polymorphisms are associated with an increased risk of developing hypertension. *Eur J Intern Med*. 2020;80:60–65. doi:10.1016/j.ejim.2020.05.014
21. Ren L, Yang X, Liu J, et al. An innovative model based on N7-methylguanosine-related lncRNAs for forecasting prognosis and tumor immune landscape in bladder cancer. *Cancer Cell Int*. 2023;23(1):85. doi:10.1186/s12935-023-02933-7
22. Wang S, Qiao C, Fang R, et al. LncRNA CASC19: a novel oncogene involved in human cancer. *Clin Transl Oncol*. 2023;25(10):2841–2851. doi:10.1007/s12094-023-03165-x